JOURNAL OF MECHANICS OF CONTINUA AND MATHEMATICAL SCIENCES
www.journalimcms.org

ISSN (Online) : 2454 -7190 Vol.-16, No.-5, May (2021) pp 1-15 ISSN (Print) 0973-8975

A HIGH GAIN AND HIGH BANDWIDTH REFLECTARRAY ANTENNA FOR 5G COMMUNICATION

Abdul Azeem[1], Shahid Bashir[2], Awais Khan[3], Sayed Sabir Shah[4]

[1,3,4] Student, Electrical Engineering Department, UET Peshawar-25000, Pakistan

[2]Asst. Professor, Electrical Engineering Department, UET Peshawar, Pakistan

[3] Lecturer, Electrical Engineering Department, UST Bannu-28100, Pakistan

[1]abdzeem8@gmail.com,[2]shahid.bashir@uetpeshawar.edu.pk,
[3]engr_awais@yahoo.com, Sayedsabirshah@gmail.com[4]

https://doi.org/10.26782/jmcms.2021.05.00001

(Received: March 15, 2021; Accepted: April 27, 2021)

Abstract

This paper presents the design of a high gain and bandwidth reflectarray for 5G networks operating in Millimeter-wave (mm Wave) at 28GHz and 38GHz. A polymer benzocylobutene (BCB) is used as substrate material having a dielectric constant of 2.65, and low tan $\delta \leq 0.0008$. The unit cell is optimized to achieve full phase reflection of 334^o over the operating band. Enhanced gain, wider bandwidth and full phase reflection are achieved by making air holes in the substrate. A 15×15 elements reflectarray based on the optimized unit cell is designed to enhance the gain. The reflectarray is excited through horn feed having a gain of 15dB with a feeding distance of 165mm and 0^0 offsets. A gain of 23dB was observed at a lower operating frequency (i.e 28GHz) and 25dB at an upper operating frequency (i.e 38GHz)with a bandwidth of 2GHz at both operating frequencies.

Keywords: Reflectarrays, gain, efficiency, unit cell, microwave, millimeter-wave, 5G

I. Introduction

Nowadays the enhancements of the latest technologies for the 5G wireless communication system is one of the main challenges for the Telecommunication industries. As 5G networks are being developed to meet the high data rate requirements for applications such as an internet of things (IoT) and wideband multimedia streaming applications. To meets, these requirements, the 5G communication system requires a wide frequency bandwidth which is possible by using high frequencies like mmWaves [XI]. However, the mmWaves have a shorter communication range due to high path loss as the atmospheric absorption of the electromagnetic waves increases at higher frequencies [XVII]. Therefore, there is a need for a high-gain efficient antenna to overcome the high path loss problem at mm-wave frequencies. Assuming the significance of the mmWaves for 5G and future networks the frequency band from (24.25-86) GHz was allotted for 5G communications [IV]. One of the possible solutions to improve gain for the 5G communications network is the two-dimensional antenna array system [IV]. However, it has a greater aperture area and narrow beamwidths. Due to the shorter

wavelength of the mmWave, the larger electrical aperture affects the physical structure of reflect array antenna. Fig.1 shows the typical structure of reflectarray consisting of a flat surface having radiating array elements. The reflector reflects back the incident rays coming from the horn feed excitation placed at some finite distance.

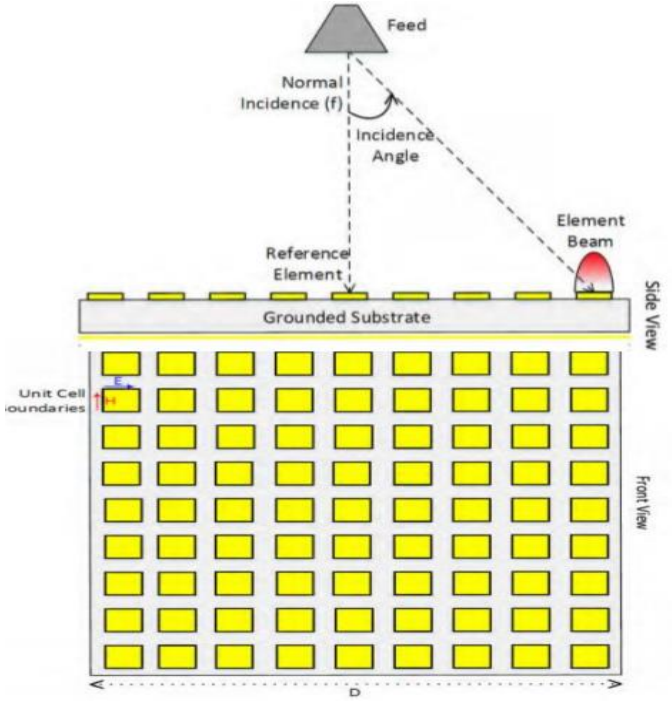

Fig.1. Typical design of reflectarray with horn feed

The lightweight planar reflectarray reflects the incoming wave like the parabolic dish reflector with the additional capability of beam scanning. Due to the curved shape, the parabolic antenna doesn't work very well in high-frequency applications [I]. However, the reflectarray antenna can be easily designed to operate at frequencies ranging from microwaves to Terahertz frequencies [V]. The design flexibility of the reflectarray makes it suitable for high gain and wideband applications. The reflectarray thin reflecting surface can provide a large phase range but it has high path loss as well as a complex design [XII]. The basic building block of a reflectarray is a resonant unit cell and its performance can be measured in terms of reflection loss, reflection phase and beam width [XI]. Its bandwidth can be controlled by changing the reflection loss and reflection phase performance. The lower the reflection loss and reflection phase the higher will be the bandwidth. The gain of reflectarray is proportional to the collective beamwidth of each unit cell patch element of the full reflectarray. The narrower the beam width, the higher will be the gain and vice versa. Therefore the combined effect of the beamwidths of all the patch elements of the unit cell will determine the overall gain of the full reflectarray model.

Larger beam width is required by the corner elements of the full array model to receive the beams coming from the horn antenna placed at some distance from the reflectarray. To achieve the high gain from the reflectarray the narrow beamwidth

elements is placed in the middle. The wide beam width elements is placed at the corners. The reasons is that the center patch elements can directly receive the beams coming from the horn antenna due to its normal incidence. Which is not possible for the corner elements and may increase the design complexity of the full model.

To obtain the high gain in a given direction, a necessary phase variation is required for each unit cell element of the reflectarray [XII]. The reflection phase variations can be achieved by elements with variable size [VI], elements with variable rotation angle [VII], the length of the stub attached to the elements and by same-size elements with variable slots [VIII]. The distance of the horn antenna from the reflecting surface is a critical parameter and has to be adjusted according to the size of the reflectarray. For proper excitation of the corner elements of the reflectarray, the feed horn distance should be increased, however, it will increase the overall structure size and will also increase the spillover losses. The f/D ratio describes the horn feed distance and D is the largest diameter of the reflectarray. To avoid the feed shadow formed due to the normal horn feed we should give an offset to the feed excitation. The type of the elements used in the unit cell and the nature of reflectarray can also affect the performance. Based upon performance characteristics, there are four types of reflectarray as shown in Fig.2.

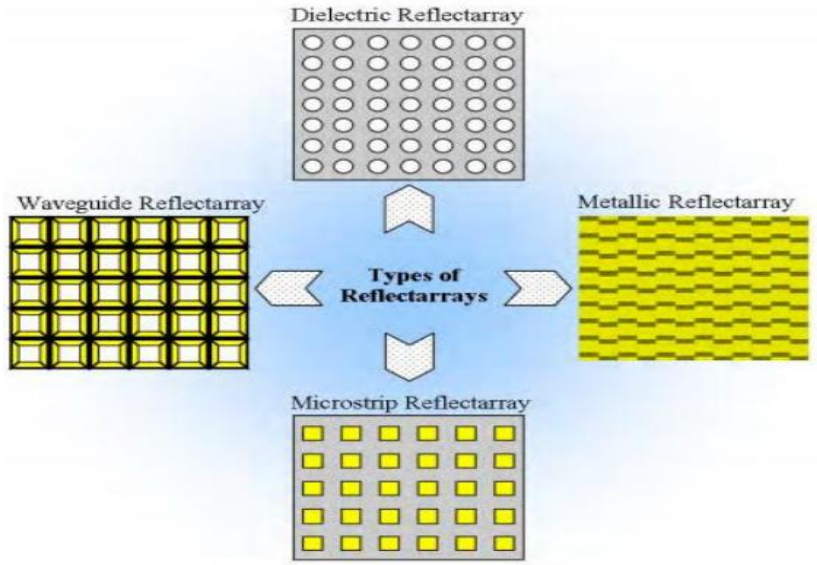

Fig.2. Different reflect-array Structures.

A dielectric reflectarray has the full dielectric layer reflections without any conducting resonant structure [VI]. Its most common type is the Dielectric Resonator Antenna (DRA) [VII], [VIII]. The same approach can be used to make the full conductor-based reflectarray [XXII]. It can enhance the gain performance by removing the dielectric loss effects particularly at the mm-Wave frequencies [XXIII]. The variable depth waveguide reflectarray antenna is another kind of metallic reflectarray [XIII]. Its phase progress distribution is correlated with the lengths of its waveguide element [II]. Removing the dielectric substrate in the metallic reflectarray is used as a loss-dropping method from resonating conductor assembly. Variable

height metallic grooves or even a metallic layer separated by the ground plane without any substrate can also be used as the full metallic reflect array antenna system. Its main purpose is to enhance the gain and efficiency by increasing the full phase reflection ranges of the reflectarray. The said antenna system can be used for mmWave applications due to its flexibility in fabrications. The Microstrip array with grounded dielectric substrate combines the best characteristics of the dielectric and the metallic reflectarray and its main advantage is to allow electronic beam steering. Waveguide reflectarray is also a type of metallic reflectarray in which arrays of the waveguide are used to reflect the incident signals. The first-ever reflectarray was an array of reflecting waveguides. The comparison of the different types of reflectarray is shown in Table.1.

Table.1: Summary of the main gain enhancement approaches (Symbols refer to H=high, M=Medium and L=Low).

Parameters	**Comparison of different types of reflectarrays**				
	Sub-Reflector	**Feeding Tactic**	**Type**		
			Microstrip	**Dielectric**	**Metallic**
Gain	H	M	M	H	H
Loss	M	M	M	L	L
Complexity	H	L	L	H	H
High-frequency compatibility	L	M	L	H	H

The miniaturized designs of dielectric and metallic reflectarrays can be a good candidate for the upcoming 5G networks if its design complexity is somehow reduced. The two-dimensional reflectarray having parallel beams has a greater gain than the linear reflectarray with the fan-beam pattern. But the greater physical aperture can reduce the performance of the full reflectarray model as beams coming from the horn antenna do not coincide with corner elements Another way to increase the gain of the reflectarray antenna is to reduce its ohmic losses due to the conductor and dielectric materials. The spillover losses and the ohmic loses are the two main degradation factors of the reflectarray. The Spillover loss depends upon the electric aperture of the feed, the distance of feed from the reflector and also on the types of excitation used, while ohmic loss is produced because of dissipation of the energy inside the material used for the fabrications. The spillover and ohmic losses are shown in Fig.3.

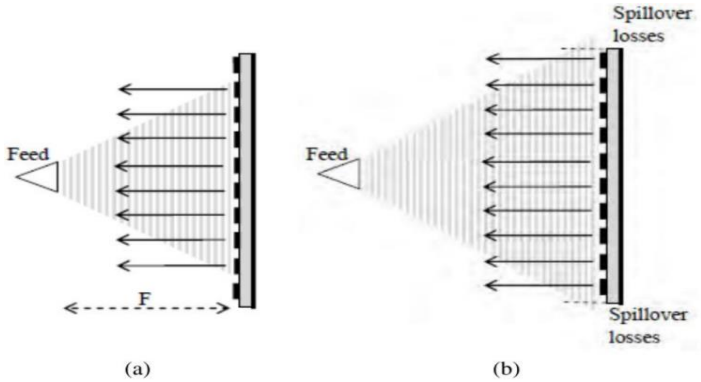

Fig.3. Reflectarray antenna with (a) Electrical aperture less than its physical aperture (b) Spillover losses.

A 5G communication system requires a high data rate of about 1-10Gbs for different types of applications [XIX]. Therefore, to fulfill this demand, the concept of mm waves was introduced, but mm waves have some limitations like high path loss due to low signal penetration power which results in a short range of the mm Waves. Hence, there is a need to design a high-gain efficient antenna to overcome this problem. There are different antennas used in literature like a parabolic antenna, phased array, two-dimensional arrays and the Massive multiple inputs multiple-output (MIMO) to decrease the high path loss of mm Waves at higher frequencies. However, due to larger size, curved shape, narrow beamwidth, design complication and the least compatibility with a higher frequency limit their wide applications. Since the reflectarray system operates at a wide range of frequencies (from Micro-Waves to the Terahertz frequencies) therefore reflectarray is a better solution for designing a high directivity/gain 5G antennas system to overcome the high path loss in mmWaves [XIV].

This paper proposes a solution for improving the gain, bandwidth, and full phase reflection of the reflectarray antenna. The proposed antenna works in 28GHz and 38GHz bands. Initially, a unit cell was designed and tested which was then converted to a full reflectarray model. A 15×15 unit cells reflect array was designed on a single layer BCB substrate. The selected material had low dielectric losses with strong stability at higher frequencies [IX]. Air holes were drilled in substate for gain, bandwidth and full phase refection optimization. The reflector is excited with a Ka-band horn to feed with an aperture area of 17.4mm×21mm and again of the 15dB and kept in the E-plane with a feeding distance of 165mm with 0^0 offsets. The proposed design was simulated in CST Microwave Studio and the results were compared with the state of the art in literature, showing improved performance in gain, bandwidth and full phase reflection behavior.

II. Antenna Designs

A. Unit Cell Design

The proposed unit cell is shown in Fig.4. A 4.3mm x4.3mm BCB polymer is used as a substrate having a dielectric constant of 2.65, and loss tangent ($\tan \delta \leq 0.0008$). The dielectric steadiness against temperature and frequency made the BCB polymer a

good material for designing the mmWave microstrip antenas [XX], [XV]. The proposed unit cell is resonating in a dual frequency band i.e 28 GHz and 38 GHz. The size of the substrate in terms of wavelength is 0.4λ at 28Ghz and 0.54λ at 38 GHz. The smaller patch element L2 defines the higher resonant frequency (38 GHz) while the larger Patch element L1 defines the lower resonant frequency (28 GHz). Similarly, the variation in scaling factor S1 varies the lower resonant frequency while that of S2 varies the higher resonant frequency. The optimized value of the distance between two adjacent patch elements is 0.22mm.

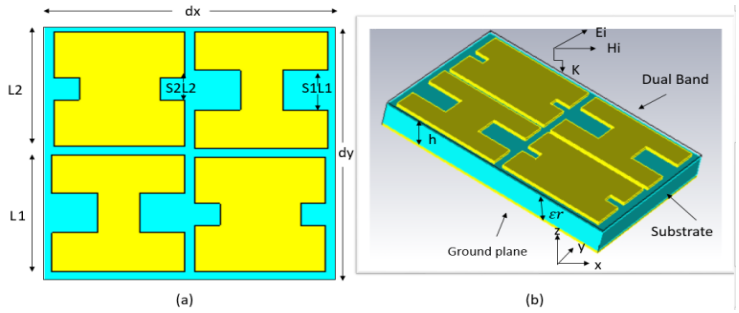

Fig.4. Unit cell layout: (a) Top view and (b) 3D view and reference system.

The scaling factor S1 is varied between 0.31-0.34 mm and S2 between 0-0.29mm. The optimized parameter values are given in table 2., S1L1 is the slot length for 28 GHz and S2L2 is the slot length for 38GHz. R is the radius of the vacuum via drilled in the substrate and p1 is the distance of vacuum via drilled in 38Ghz metallic patch from the center of the patch. The reflection phase of the unit cell as well as a full reflectarray model can be controlled by varying the diameter of air-filled holes in the substrate, and can also be varied by changing the slot lengths S1L1 and S2L2.

Table.2: Dimension of the Unit Cell parameters

Parameters	Dimensions(mm)	Parameters	Dimensions(mm)
DX	4.3	Ts	0.261
DY	4.3	Tc	0.02
S1	0.3	D	0.22
S2	0.13	S	0.2
L1	1.95	P	0.1
L2	1.91	R	0.13
S1L1	0.7	S2L2	0.3

B. Mushroom EBG Unit Cell

The proposed fractal patch design is derived from the first iteration of the square fractal patch element shown in Fig.5.

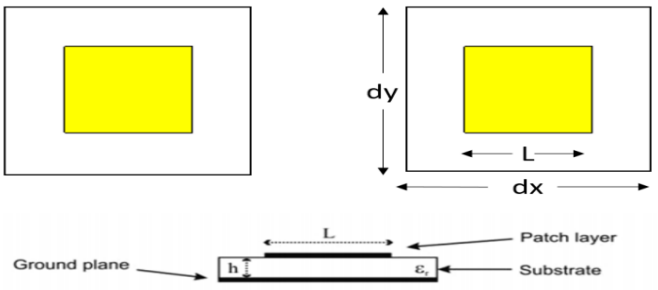

Fig.5. Square patch generator and its Dimension.

C. 1ST Iteration Square Patch

Our proposed unit cell design is taken from the single square shape fractal patch (i.e square shape Minkowski patch unit cell) by the first iteration method. The unit cell and the full reflectarray model can be optimized in terms of gain, bandwidth and reflection phase by inserting air holes in the substrate material. Our proposed unit cell structure is shown in Fig.6.

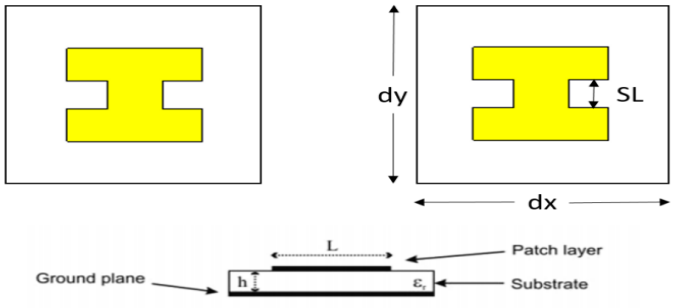

Fig.6. Ist iteration Patch with its dimension.

III. Results and Discussion

A. Mushroom EBG Unit Cell

The reflection phase behavior of the Mushroom EBG is shown in Fig.7.

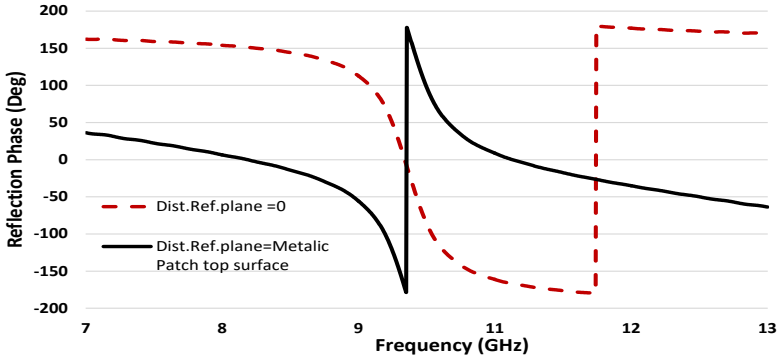

Fig.7. Reflection Phase Behaviour of Mushroom EBG.

It can be observed in Fig.7 that the structure has the $\pm 180^0$ phase variation at the low and high frequencies and has the zero phase shift at the resonant frequency. The phase reflection between $\pm 90^0$ represents the AMC behavior of the EBG at the cut-off frequency.

B. 1ST Iteration Square Patch

Our proposed unit cell design consists of two interchangeably square fractal patches operating at specific resonant frequencies (f1=28Ghz and f2=38Ghz). The design of the single fractal patch is derived from the first iteration of the fixed-length square Minkowski fractal patch. The reflection phase behavior of our proposed unit cell is shown in Fig.8.

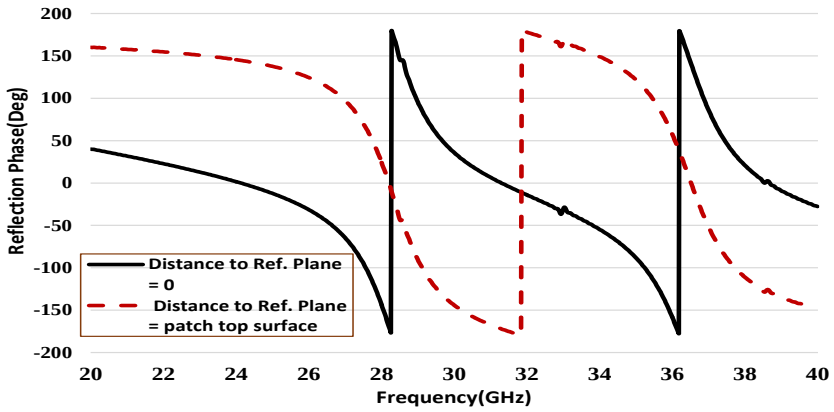

Fig.8. Reflection Phase Behavior of Proposed Unit Cell

It can be observed from the reflection phase graph of our proposed unit cell in fig 8 that the structure has $\pm 90^0$ phase shift at lower and higher frequencies and shows the PEC behavior at low and high frequencies. The unit cell does not have zero phase shift at the lower and higher resonant frequencies (i.e 28Ghz and 38Ghz). The proposed unit cell can be further parameterized to get $\pm 90^0$ phase shift at the lower and higher frequencies and to obtain zero phase shift at both resonant frequencies(i.e 28Ghz and 38Ghz). To get high gain, bandwidth and even a good full phase reflection from the unit cell as well as the full reflectarray model, the proposed structure must show the AMC behavior at both the resonant frequencies.

C. Parametric Analysis of the Proposed Unit Cell

The full phase reflection at each resonant frequency (i.e f1=28 GHz and f2=38 GHz) can be varied by changing the scaling factors (i.e S1 and S2) while keeping the fractal patch size L1×L2 unchanged. Both the scaling factors S1 and S2 are varied to get the full phase reflection at both resonance frequencies. The scaling factor associated with 38 GHz patch S2 is varied from 0.19-1mm in steps as shown in Fig.9 (a to d).To get the desire reflection phase at the both resonant frequencies (i.e at 28 GHz and 38 GHz) the scaling factor associated with smaller square patch (i.e 38Ghz patch) S2 was parameterized in steps, i.e from 0.6-1mm in Fig.9(a), from 0.2mm- 0.5mm in Fig.9(b), from 0.23mm-0.35mm in Fig.9(c) and finally from 0.12mm- 0.21mm in

Fig.9 (d) .However the optimized value of S2 =0.27mm gives the minimum reflection phase behavious at both resonant frequencies.

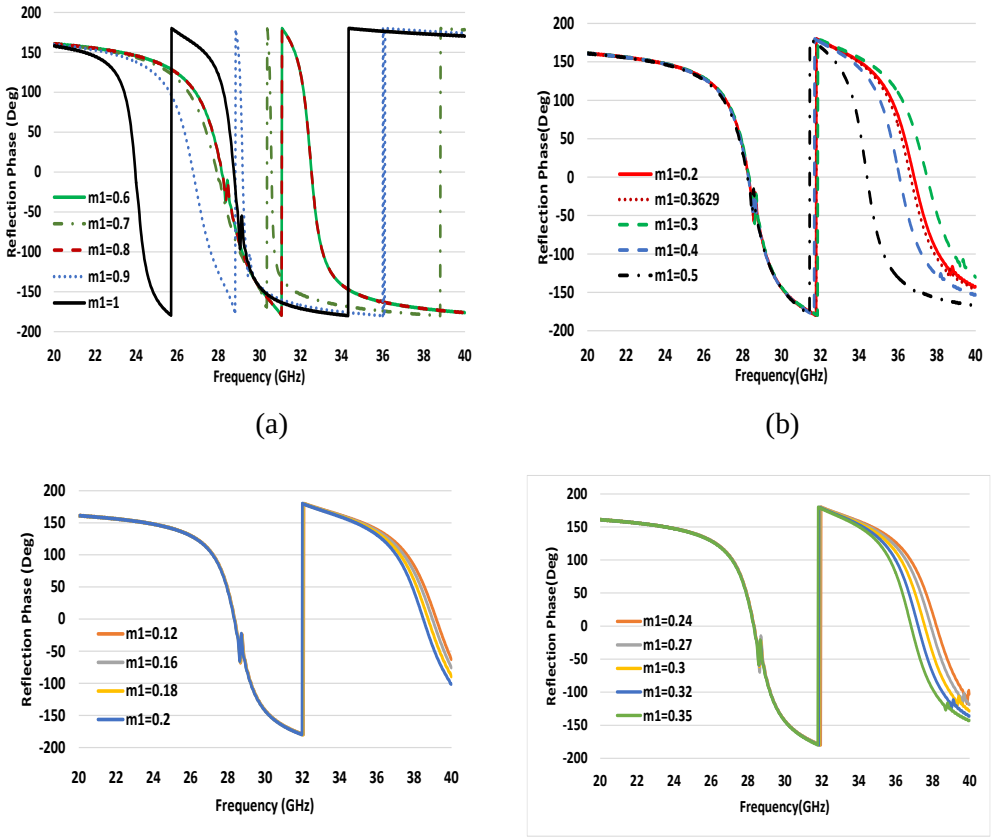

Fig.9. Reflection Phase versus frequency (a) L1=1.95mm,m1=(0.2-0.5mm), L2 = 1.91mm (b) L1 = 1.95mm, m1 = (0.230.35mm) (c) L1 = L1 = 1.95mm, m1 = (0.12-0.2 mm), L2 = 1.91 mm.

It can be concluded from the parametric analysis that a minimum phase shift of -0.8^0 was observed at the 38GHz resonance frequency and a phase shift of $-2.18^0$was observed at 28GHz resonance frequency for S2=0.27mm. The reflection phase graph shows good AMC behavior. The reflection phase graph of the unit as well as the full reflectarray can be further optimized by drilling an air hole inside the substrate material. Using this novel concept, a 0^0 phase shift can be obtained at both resonance frequencies and the reflection phase graph shows even better AMC behavior which can be observed in Fig.10.

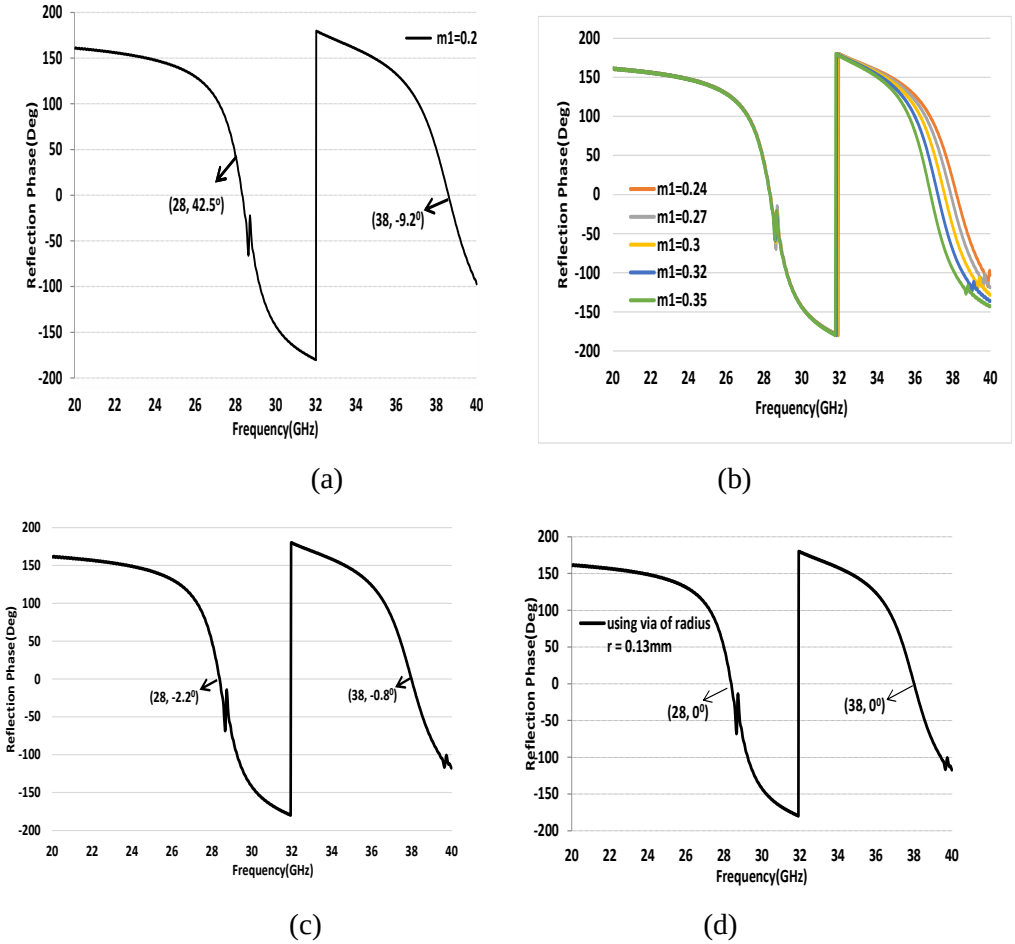

Fig.10. Reflection Phase versus frequency (a) L1=1.95mm,L2=1.91mm,m1=0.2mm,S1=0.34mm (b) L1=1.95mm,L2=1.91mm,m1=(0.1-0.35mm),S1=0.34mm,(c) L1=1.95mm,L2=1.91mm,m1=0.27mm,S1=0.34mm,(d) Using dual substrate material.

Moreover, the reflection amplitude Vs Frequency behavior can be shown in Fig.11

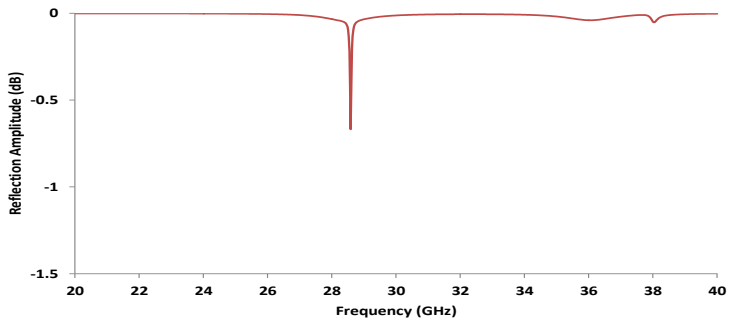

Fig.11. Reflection Amplitude Vs Frequency

The dual band resonance was obtained by using two pairs of smaller square fractal patches inside the proposed unit cell. the scaling factor S2 defines the the higher resonant frequency while that of S1 defines the lower resonance frequency, keeping the patch size (i.e L1 and L2) constant. Unit cells with offset feed can best be simulated in the frequency domain. A negligible phase variation is observed as compared to normal incidence i.e (θ=0^0) as shown in Fig.12.

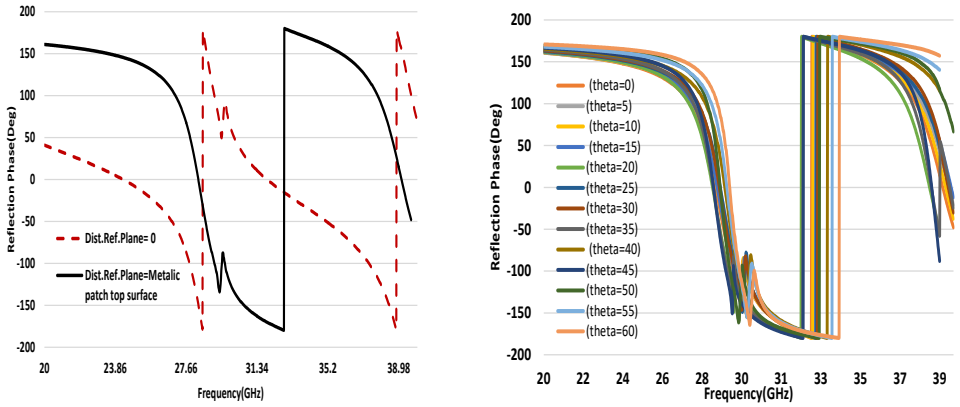

(a) (b)

Fig.12. Reflection Phase versus Frequency(a) Frequncy Domain (b) Offset Feed.

D. Full Reflectarray Design

i. 3×11 Reflectarray Design

A dual-band 3×11 elements full reflectarrays is designed and tested. The reflector is fed with a Ka-band horn antenna having 15dB gain and aperture dimensions of 17.4mm×21mm placed in the yz-plane at a distance of 165mm with a normal incidence as shown in Fig.13.

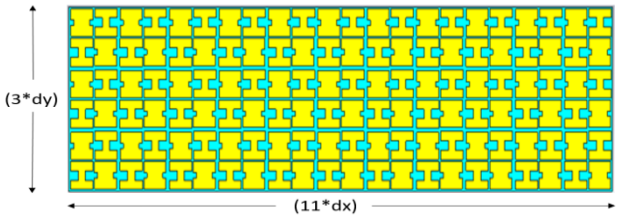

Fig.13. 3×11 Reflectarray Pattern

Since our proposed unit cell as well as the full reflectarray shows dual-band behavior. The observed gain at both resonant frequencies (i.e 28 GHz and 38 GHz) for the full reflectarray model is 17dB and 16.5 dB. Although the structures proposed in the literature have not been properly optimized in terms of bandwidth, gain, and full phase reflection. Our proposed structure optimized in terms of bandwidth, gain and the full phase reflection by using a novel technique of drilling circular air holes in the

substrate material. The proposed model was simulated in CST Micro Studio for Gain, Bandwidth and Reflection Phase. The observed gain at both resonant frequencies (i.e 28 GHz and 38GHz) is 17dB and 19dB as shown in Fig.13. The reflectarray model with a drilled circular air hole in the substrate is also simulated for some offset feed. A negligible phase variation is observed as compared to normal incidence i.e (θ=0^0) as shown in Fig.14.

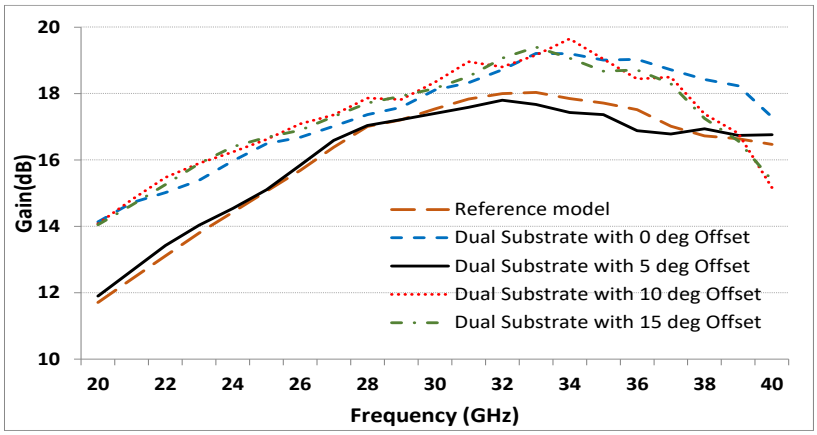

Fig.14. Gain versus frequency

ii. 15×15 Reflectarray Design

Finally a 15×15 elements full reflectarray is also designed and simulated. The reflector is fed with a Ka-band horn antenna having 15dB gain and aperture dimensions of 17.4mm×21mm located in the yz-Plane(E-Plane) at a distance of 165mm with normal incidence shown in Fig.15.The observed gain at the lower cutoff frequency is 23dB and 25dB for the upper frequency with a bandwidth of 2GHz and the full phase reflection of 334^0 for both the cutoff frequencies. The reflection phase and gain versus frequency graphs are shown in Fig.16.

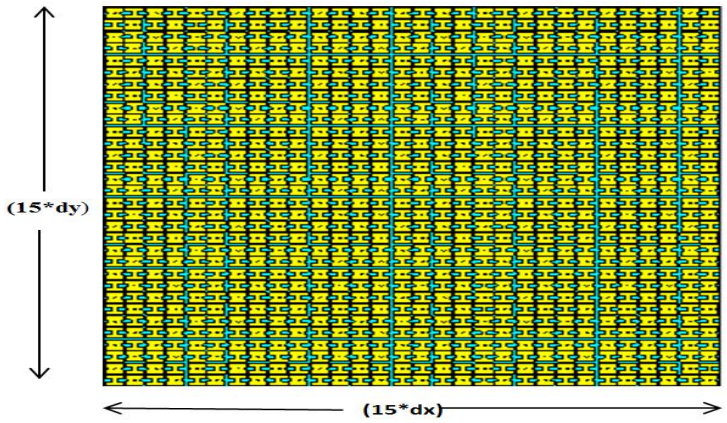

Fig.15. 3×11 Reflectarray Pattern

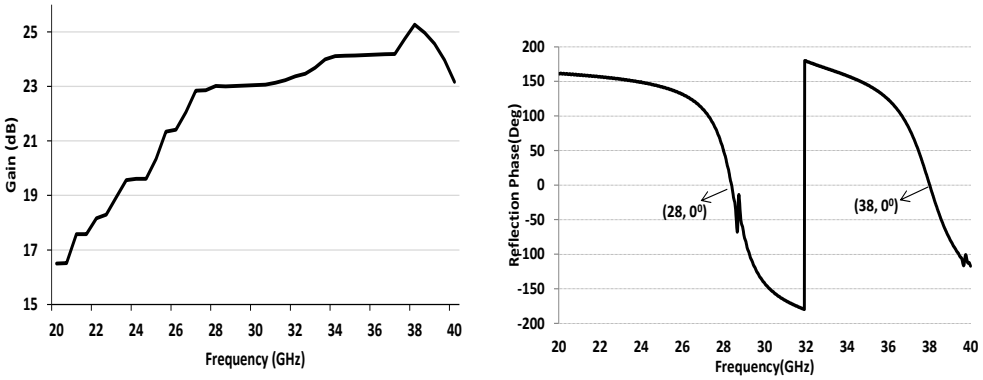

(a) (b)

Fig.16. (a) Gain versus frequency (b) Reflection phase versus frequency.

Table.4: Comparison with related work published in the literature (where f_1 & f_2 are the lower and upper cut off frequencies)

References	Full phase reflection	Band	Bandwidth (GHz)		Gain(dB)		Size
			at f_1	at f_2	at f_1	at f_2	
[1]	332^0	Dual	0.955 (at 28GHz)	1 (at 38GHz)	20 (at 28GHz)	24 (at 38GHz)	(0.04 * 0.05) λ
[21]	332^0	Dual	0.955 (at 28GHz)	1 (at 38GHz)	NA	NA	(0.04 * 0.05) λ
[19]	300^0	Single	1.8% (at 10GHz)	NA	NA	NA	(0.3*0.3) λ
[20]	305^0	Single	1% (at 8.7GHz)	NA	NA	NA	(0.6*0.6) λ
[21]	320^0	Single	1.2%(at 8.8GHz)	NA	NA	NA	(0.3*0.3) λ
This Work	334^0	Dual	2	2	23	25	(0.03 * 0.03) λ

Table.4 shows a comparison of our proposed model with the related designs already published in the literature. The comparison was made in terms of size, Gain, Bandwidth and reflection phase behavior. It can be observed that our proposed design has a more compact size, a higher gain, bandwidth and a greater full phase reflection.

IV. Conclusion

In this research, a new technique of inserting air holes in the substrate is used to improve the gain, bandwidth and full phase reflection of reflectarrays. The unit cell of a reflectarray is first parametrized and optimized for improved reflection phase behavior. The complete reflectarray design is then simulated by a horn feed antenna. A 15×15 single layer dual-band reflectarray with a BCB substrate having air holes is designed and simulated in CST MW studio. The reflectarray is fed with a Ka-band horn antenna having 15dB gain placed at a distance of 165mm with normal incidence. The proposed design is optimized for high gain, bandwidth and the full phase reflection and gives a gain of 23 dB at 28GHz and 25 dB at 38GHz with a bandwidth of 2Ghz and have the full phase reflection of 334^0 at both bands.

Conflict of Interest:

There was no relevant conflict of interest regarding this paper.

References

I. D. Spectrum, "Euro-5g – Supporting the European 5G Initiative," 2017.

II. D. G. Berry, R. G. Malech, and W. A. Kennedy, "The Reflectarray Antenna," *IEEE Trans. Antennas Propag.*, vol. 11, no. 6, pp. 645–651, 1963, doi: 10.1109/TAP.1963.1138112.

III. D. Oloumi, S. Ebadi, A. Kordzadeh, A. Semnani, P. Mousavi, and X. Gong, "Miniaturized reflectarray unit cell using fractal-shaped patch-slot configuration," *IEEE Antennas Wirel. Propag. Lett.*, vol. 11, pp. 10–13, 2012, doi: 10.1109/LAWP.2011.2181478.

IV. F. Boccardi, T. L. Marzetta, and B. Labs, "Five Disruptive Technology Directions for 5G," no. February, pp. 74–80, 2014.

V. M. Hashim Dahri and M. Y. Ismail, "Performance analysis of reflectarray resonant elements based on dielectric anisotropic materials," *Procedia Eng.*, vol. 53, pp. 203–207, 2013, doi: 10.1016/j.proeng.2013.02.027.

VI. M. Abd-Elhady, W. Hong, and Y. Zhang, "A Ka-band reflectarray implemented with a single-layer perforated dielectric substrate," *IEEE Antennas Wirel. Propag. Lett.*, vol. 11, pp. 600–603, 2012, doi: 10.1109/LAWP.2012.2201128.

VII. M. H. Jamaluddin *et al.*, "Design, fabrication and characterization of a dielectric resonator antenna reflectarray in ka-band," *Prog. Electromagn. Res. B*, vol. 25, no. 25, pp. 261–275, 2010, doi: 10.2528/PIERB10071306.

VIII. M. H. Jamaluddin *et al.*, "A dielectric resonator antenna (DRA) reflectarray," *Eur. Microw. Week 2009, EuMW 2009 Sci. Prog. Qual. Radiofreq. Conf. Proc. - 39th Eur. Microw. Conf. EuMC 2009*, vol. 6164, no. October, pp. 25–28, 2009, doi: 10.1109/EUMC.2009.5296579.

IX. M. H. Dahri, M. H. Jamaluddin, M. I. Abbasi, and M. R. Kamarudin, "A Review of Wideband Reflectarray Antennas for 5G Communication Systems," *IEEE Access*, vol. 5, pp. 17803–17815, 2017, doi: 10.1109/ACCESS.2017.2747844.

X. Muhammad Sohaib Jamal, Samad Baseer, Iqtidar Ali, Farooq Faisal. : 'ANALYSIS OF CHANNEL MODELLING FOR 5G MMWAVE COMMUNICATION'. J. *Mech. Cont.& Math. Sci.*, Vol.-15, No.-9, September (2020) pp 278-293. DOI : 10.26782/jmcms.2020.09.00023

XI. S. Costanzo, F. Venneri, A. Borgia, and G. Di Massa, "A single-layer dual-band reflectarray cell for 5G communication systems," *Int. J. Antennas Propag.*, vol. 2019, pp. 8–11, 2019, doi: 10.1155/2019/9479010.

XII. S. W. Oh, C. H. Ahn, "Reflect-array element using variable ring with slot on ground plane," *Electron. Lett.*, vol. 45, doi: 10.1049/el.2009.2693.

XIII. S. V. Polenga, A. V. Stankovsky, R. M. Krylov, A. D. Nemshon, Y. A. Litinskaya, and Y. P. Salomatov, "Millimeter-wave waveguide reflectarray," *2015 Int. Sib. Conf. Control Commun. SIBCON 2015 - Proc.*, pp. 0–3, 2015, doi: 10.1109/SIBCON.2015.7147335.

XIV. S. Costanzo, F. Venneri, and G. Di Massa, "c," *13th Eur. Conf. Antennas Propagation, EuCAP 2019*, no. EuCAP, pp. 1–3, 2019.

XV. S. Costanzo, I. Venneri, G. Di Massa, and A. Borgia, "Benzocyclobutene as Substrate Material for planar millimeter-wave structures: Dielectric characterization and application," *J. Infrared, Millimeter, Terahertz Waves*, vol. 31, no. 1, pp. 66–77, 2010, doi: 10.1007/s10762-009-9552-0.

XVI. S. Costanzo, F. Venneri, A. Borgia, I. Venneri, and G. Di Massa, "60 GHz microstrip reflectarray on a benzocyclobutene dielectric substrate," *IET Sci. Meas. Technol.*, vol. 5, no. 4, pp. 134–139, 2011, doi: 10.1049/iet-smt.2010.0132.

XVII. S. Costanzo and F. Venneri, "Miniaturized fractal reflectarray element using fixed-size patch," *IEEE Antennas Wirel. Propag. Lett.*, vol. 13, pp. 1437–1440, 2014, doi: 10.1109/LAWP.2014.2341032.

XVIII. S. Costanzo, F. Venneri, G. Dimassa, A. Borgia, A. Costanzo, and A. Raffo, "Fractal reflectarray antennas: State of art and new opportunities," *Int. J. Antennas Propag.*, vol. 2016, 2016, doi: 10.1155/2016/7165143.

XIX. T. S. Rappaport *et al.*, "Millimeter wave mobile communications for 5G cellular: It will work!," *IEEE Access*, vol. 1, pp. 335–349, 2013, doi: 10.1109/ACCESS.2013.2260813.

XX. T. S. Rappaport, Y. Xing, G. R. MacCartney, A. F. Molisch, E. Mellios, and J. Zhang, "Overview of Millimeter Wave Communications for Fifth-Generation (5G) Wireless Networks-With a Focus on Propagation Models," *IEEE Trans. Antennas Propag.*, vol. 65, no. 12, pp. 6213–6230, 2017, doi: 10.1109/TAP.2017.2734243.

XXI. Tallapalli Chandra Prakash, Srinivas Samala, Kommabatla Mahender. : 'MULTICARRIER WAVEFORMS FOR ADVANCED WIRELESS COMMUNICATION'. *J. Mech. Cont.& Math. Sci*., Vol.-15, No.-7, July (2020) pp 252-259. DOI : 10.26782/jmcms.2020.07.00020

XXII. W. An, S. Xu, F. Yang, and S. Member, "A Metal-Only Re fl ectarray Antenna Using Slot-Type Elements," vol. 13, pp. 1553–1556, 2014.

XXIII. W. Lee, M. Yi, J. So, and Y. J. Yoon, "Non-resonant conductor reflectarray element for linear reflection phase," *Electron. Lett.*, vol. 51, no. 9, pp. 669–671, 2015, doi: 10.1049/el.2015.0194.